References and Notes

1. T. Someya, H. Akiyama, H. Sakaki, *Phys. Rev. Lett.* **74**, 3664 (1995).
2. F. Vouilloz *et al.*, *Phys. Rev. B* **57**, 12378 (1998).
3. H. Akiyama, T. Someya, H. Sakaki, *Phys. Rev. B* **53**, R4229 (1996).
4. P. Ils *et al.*, *Phys. Rev. B* **51**, 4272 (1995).
5. J. Hasen *et al.*, *Nature* **390**, 54 (1997).
6. X. Duan, C. M. Lieber, *Adv. Mater.* **12**, 298 (2000).
7. M. S. Gudiksen, C. M. Lieber, *J. Am. Chem. Soc.* **122**, 8801 (2000).
8. M. S. Gudiksen, J. Wang, C. M. Lieber, *J. Phys. Chem. B* **105**, 4062 (2001).
9. Excitation light (488 or 514 nm) was focused by an objective (NA = 0.7) to a ~30-μm diameter spot at ~1.0 kW/cm^2 on the quartz substrate with nanowires dispersed on it. A λ/2 wave plate was used to change the polarization of excitation light. The resulting PL was collected by the same objective, filtered to remove excitation light, focused, and either imaged or spectrally dispersed onto a liquid nitrogen–cooled CCD. To determine the emission polarization, a Glan-Thompson polarizer was placed in front of the spectrometer to detect emission intensities.
10. S. A. Empedocles, D. J. Norris, M. G. Bawendi, *Phys. Rev. Lett.* **77**, 3873 (1996).
11. PL spectra exhibit a diameter-dependent shift in the PL emission energy from the bulk band gap of InP (1.35 eV) for diameters ≤20 nm. Detailed studies show that diameter-dependent spectra collected from nanowires at room temperature and ~7 K can be explained in terms of radial quantum confinement. Giant polarization anisotropy is observed in nanowires with diameters from 10 to 50 nm at room temperature and 7 K.
12. M. S. Gudiksen, J. Wang, C. M. Lieber, in preparation.
13. L. D. Landau, E. M. Lifshitz, L. P. Pitaevskii, *Electrodynamics of Continuous Media* (Pergamon, Oxford, 1984), pp. 34–42.
14. X. Duan, Y. Huang, Y. Cui, J. Wang, C. M. Lieber, *Nature* **409**, 66 (2001).
15. Y. Huang, X. Duan, Q. Wei, C. M. Lieber, *Science* **291**, 630 (2001).
16. Y. Cui, C. M. Lieber, *Science* **291**, 851 (2001).
17. S. Ura, H. Sunagawa, T. Suhara, H. Nishihara, *J. Lightwave Tech.* **6**, 1028 (1988).
18. C. J. Chen, K. K. Choi, L. Rokhinson, W. H. Chang, D. C. Tsui, *Appl. Phys. Lett.* **74**, 862 (1999).
19. M. Bass *et al.*, *Handbook of Optics* (McGraw Hill, New York, 1995), pp. 17.1–17.29.
20. These very small devices could prove useful for high-speed detection because the response times of semiconductor photodetectors can be limited by their resistance-capacitance (RC) time constants (*19*). On the basis of improved nanowire–metal contacts (10 kilohm) and intrinsically small capacitances (~10^{-17} F) (*21*), RC time constants on the order of 100 fs can be realized. By decreasing the electrode separation to ensure direct collection of photogenerated carriers, detection speeds on the order of 100 fs or less may be realized with these nanoscale detectors.
21. Y. Cui, X. Duan, J. Hu, C. M. Lieber, *J. Phys. Chem. B* **104**, 5213 (2000).

22. We thank L. Lauhon and H. Park for helpful discussions. M.S.G. thanks the NSF for predoctoral fellowship support. C.M.L. acknowledges support of this work by the Office of Naval Research and Defense Advanced Projects Research Agency.

8 May 2001; accepted 24 August 2001

Time-Resolved Measurement of Dissipation-Induced Decoherence in a Josephson Junction

Siyuan Han,[1]* Yang Yu,[1] Xi Chu,[2] Shih-I Chu,[2] Zhen Wang[3]

We determined the dissipation-induced decoherence time (DIDT) of a superconducting Josephson tunnel junction by time-resolved measurements of its escape dynamics. Double-exponential behavior of the time-dependent escape probability was observed, suggesting the occurrence of a two-level decay-tunneling process in which energy relaxation from the excited to the ground level significantly affects the escape dynamics of the system. The observation of temporal double-exponential dependence enables direct measurements of the DIDT, a property critical to the study of quantum dynamics and the realization of macroscopic quantum coherence and quantum computing. We found that the DIDT was $\tau_d > 11$ μs at $T = 0.55$ K, demonstrating good prospects for implementing quantum computing with Josephson devices.

Use of solid-state devices (SSD) is regarded as one of the most promising approaches for the development of quantum computers (QC), due to the relative ease of circuit design, fabrication, and scaling up (*1–10*). However, coupling between SSD and the environment results in dissipation, and hence decoherence. Here, decoherence refers to processes that lead to exponential decay of superposition states into incoherent mixtures. The severity of decoherence is characterized by the decoherence time—the time constant τ of the exponential decay. Both dissipation (with decoherence time τ_d) and phase relaxation (with τ_φ) lead to decoherence (*11–15*). Realization of QC will depend critically on our ability to create and preserve coherent superposition states so that decoherence presents the most fundamental obstacle (*11–16*). One way to increase the decoherence time in SSD is to use superconducting qubits (SQ) based on superconducting quantum interference devices (SQUIDs) (flux qubits) or single-pair tunneling devices (charge qubits) (*3–10*). For both types of SQ, the Josephson junction is the key element and it is the dissipation of the junctions that will set the limit on decoherence time. Furthermore, for SQUID qubits τ_d^{-1} and τ_φ^{-1} are predicted to be proportional to the level of dissipation (*17, 18*). Therefore, the feasibility of implementing QC with SQ depends on whether dissipation in Josephson junctions can be made sufficiently low to keep the error rate to a tolerable level. However, experimental determination of either τ_d or τ_φ is extremely difficult for superconducting devices because in each measurement only a single device, rather than an ensemble of identical devices, is available for signal detection. Furthermore, prior to this work no time-domain measurement with resolution comparable to the decoherence time scale of SQ has been demonstrated. For these reasons, no time-resolved measurement of τ_d (or τ_φ) has been reported yet. Recent attempts to determine the effective damping resistance of a Josephson junction in a SQUID were inconclusive due to the questionable method of data analysis used and the indirect nature of the measurement technique (*19, 20*). We present time-resolved measurements of τ_d in a NbN/AlN/NbN Josephson junction. The measured decoherence time, $\tau_d > 10$ μs at $T = 0.55$ K, corresponds to a qubit quality factor $\tau_d/\tau_{op} \sim 10^4$ (where $\tau_{op} \sim 1$ ns is the typical gate time of SQUID qubits), demonstrating strong potential for QC employing NbN SQUID qubits (*12*).

The equation of motion for a current biased Josephson junction, $Cd^2\Phi/dt^2 + R^{-1}d\Phi/dt = -\partial U/\partial\Phi$, is homologous to that of a particle of mass C moving in a washboard potential $U(\Phi) = -I_b\Phi - E_J\cos(2\pi\Phi/\Phi_0)$ with damping constant R^{-1}, where C is the junction capacitance, R is the shunt resistance, $\Phi_0 \equiv h/2e$ is the flux quantum, $E_J \equiv I_c\Phi_0/2\pi$ is the magnitude of maximum Josephson coupling energy, I_c is the critical current of the junction, I_b is the bias current, and $\Phi \equiv (\varphi/2\pi)\Phi_0$, where φ is the phase difference across the junction. For $i_b \equiv I_b/I_c < 1$, the potential has a series of metastable wells. The dc voltage across the junction is zero when the particle is trapped in a potential well. The depth of the potential well decreases as i_b is increased and becomes zero for $i_b \geq 1$. In the presence of thermal/quantum fluctuations, a junction initially trapped in the zero-voltage state can escape from the potential well to enter the finite-voltage state.

Previous experiments have demonstrated

[1]Department of Physics and Astronomy, University of Kansas, Lawrence, KS 66045, USA. [2]Department of Chemistry, University of Kansas, Lawrence, KS 66045, USA. [3]Kansai Advanced Research Center, Communication Research Laboratory, Ministry of Posts and Telecommunications, 588-2 Iwaoka, Iwaoka-cho, Nishi-ku, Kobe, 651-24 Japan.

*To whom correspondence should be addressed. E-mail: han@ku.edu

that when damping is sufficiently low the junction is a macroscopic quantum object with quantized energy levels (*21, 22*). For weak damping, the quality factor of the junction is $Q \equiv \omega_p RC$, where $\omega_p = (2\pi I_c/C\Phi_0)^{1/2}(1 - i_b^2)^{1/4}$ is the plasma frequency of the junction. The primary effect of weak damping ($Q \gg 1$) on the intrawell dynamics of the junction is that at low temperature ($k_BT \ll$ level separation) the width of an excited level $|n\rangle$, with energy E_n, is given approximately by $\delta E_n \simeq E_n/Q$ (*23, 24*). In thermal equilibrium, escape from the potential well is dominated by macroscopic quantum tunneling (MQT) from the ground level $|0\rangle$ for $T \ll \hbar\omega_p/k_B$. By contrast, in a nonequilibrium state the excited levels could have excessive population that can be created by rapidly ramping up the bias current and/or applying dc pulse or microwave excitations. For nonequilibrium states, tunneling from excited levels can be important to the escape process. In particular, tunneling from overpopulated excited levels can dominate the escape process even at temperatures much higher than the crossover temperature for the ground state MQT, as demonstrated by recent experiments (*25*).

At low temperatures, the simplest nonequilibrium escape process that involves tunneling from both the ground and the excited levels is the two-level decay-tunneling (TLDT) process (Fig. 1), which allows a direct measurement of τ_d. For a junction with probability $\rho_{11}(0)$ in the level $|1\rangle$ at $t = 0$, the probability of finding it remaining in the zero-voltage state at $t > 0$ is given by

$$P(t) = (1 - \gamma)e^{-\Gamma_0 t} + \gamma e^{-\Gamma' t} \qquad (1)$$

where $\Gamma' \equiv \Gamma_1 + \Gamma_d$, $\Gamma_0(\Gamma_1)$ is the escape rate from the level $|0\rangle$ ($|1\rangle$) out of the potential well, Γ_d is the spontaneous decay rate from $|1\rangle$ to $|0\rangle$, and $\gamma \equiv \rho_{11}(0)[1 - \Gamma_d/(\Gamma' - \Gamma_0)]$ is bounded between zero and unity. The transition from $|0\rangle$ to $|1\rangle$, which is negligible at low temperature, was not included in the model.

The interlevel decay rate,

$$\Gamma_d = \frac{2\pi(E_1 - E_0)}{\hbar}\frac{R_Q}{R}|\langle 0|\phi|1\rangle|^2 \times \left[1 + \coth\left(\frac{E_1 - E_0}{2k_BT}\right)\right] \qquad (2)$$

is $\propto R^{-1}$ (*16*). Where, $E_1 - E_0$ is the energy separation between levels $|0\rangle$ and $|1\rangle$, $R_Q \equiv h/4e^2$ is the resistance quantum, and $\phi \equiv \varphi/2\pi$. For quadratic potentials $\Gamma_d \rightarrow E_1/Q$ in the limit of $k_BT \ll E_1$ as expected (*23, 24*). The ϕ matrix element and $E_1 - E_0$ can be calculated from the independently measured junction parameters so that R can be determined directly from Γ_d.

The most distinctive feature of the TLDT process is the double-exponential decay of $P(t)$ (Eq. 1). The time-dependent escape probability, $P_{esc}(t) = 1 - P(t)$, has two characteristic time scales: the average lifetimes, $\tau_0 \equiv 1/\Gamma_0$ and $\tau' \equiv 1/\Gamma'$, of the junction in levels $|0\rangle$ and $|1\rangle$, respectively. However, whether the double-exponential time dependence can be observed depends crucially on the relative magnitude of the three rate constants. Qualitatively speaking, if the junction is initially in $|1\rangle$ and $\Gamma_d \gg \Gamma_1$ (i.e., $\gamma \ll 1$) the system will decay rapidly to $|0\rangle$ before having a chance to escape from $|1\rangle$. Thus, only the slow component of the double-exponential behavior of $P_{esc}(t)$ can be observed. In the opposite limit of $\Gamma_d \ll \Gamma_1$ (i.e., $\gamma \approx 1$) the system mainly escapes from $|1\rangle$ before decaying to $|0\rangle$. Therefore, only the fast component can be observed. Because junction resistance increases as temperature is lowered, one expects the former (latter) behavior at high (low) temperatures. The situation is quite different for the intermediate temperature regime where Γ_d is comparable to Γ_1 (i.e., $\gamma \approx 0.5$). In this case, the probabilities of escaping out of the zero-voltage state from either $|0\rangle$ or $|1\rangle$ are approximately equal and the double-exponential behavior should be observed clearly, from which three parameters, γ, Γ_0, and Γ', can be extracted directly from the measured $P_{esc}(t)$. Although τ_d cannot be determined exactly from $P_{esc}(t)$ measurement due to the incomplete knowledge about $\rho_{11}(0)$, its lower bound is set by $1/\Gamma'$ since $\Gamma' > \Gamma_d$.

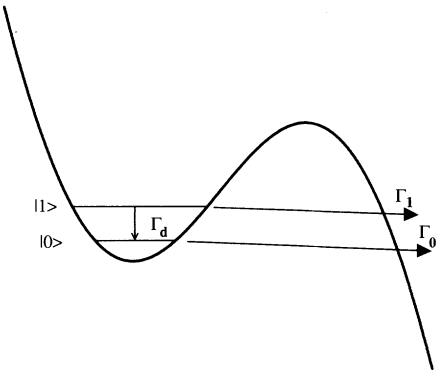

Fig. 1. Illustration of the TLDT process described in the text.

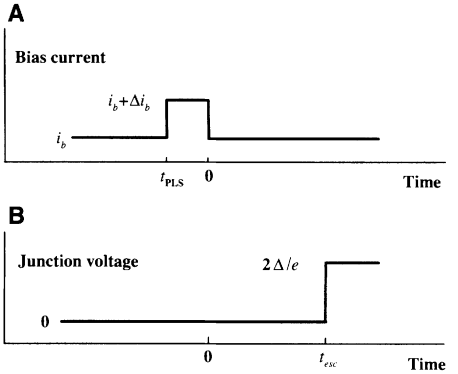

Fig. 2. (**A**) A schematic of the timing of the constant and "dc pulse" current applied to the junction. (**B**) The junction's voltage response, and the definition of t_{esc}.

In our experiment, we used a 10 μm^2 by 10 μm^2 NbN/AlN/NbN tunnel junction to measure the time-dependent escape probability at 10 mK $\leq T \leq$ 4.25 K. The junction was fabricated on a single-crystal MgO substrate at ambient temperature (*26*). The critical temperature of the junction was ~16 K. The gap energy Δ and normal state resistance R_n were 2.7 meV and 20 ohms, respectively. The critical current, I_c = 150.86 μA, was determined from switching current distribution measurements. I_c remained essentially constant below 4.2 K. The plasma frequency and capacitance of the junction, determined from resonant activation measurements (*21*), were $\omega_p/2\pi$ = 18.195 ± 0.001 GHz at 4.2 K and C = 5.8 ± 0.6 pF. C was much greater than the parasitic capacitance (<0.3 pF) of the leads within the junction's electromagnetic horizon (*27*), so the impedance loading effect of the leads was negligible. The junction was embedded in a superconducting microstrip resonator with a fundamental frequency of ~40 GHz so that it was effectively decoupled from the leads at $\omega < \omega_p$. The junction was mounted in a helium-filled oxygen-free copper cell, which was thermally anchored to the mixing chamber (MC) of a dilution refrigerator. All leads to the cell were filtered with electromagnetic interference (EMI) filters at room temperature, low-pass filters at 1.4 K, and cryogenic microwave filters (*28*) at MC temperature. A semirigid cryogenic coaxial cable, with 20 dB attenuators at 1 K plate and MC, couples microwave or dc pulses to the junction. Battery-powered low-noise preamplifiers were used to monitor the bias current and junction voltage. A solid copper shielded room, double-shielded cables, and shielded metal connectors formed a continuous conducting enclosure that extended from the sample to the battery-powered part of the setup. The computer and ac-powered instruments were placed outside the shielded room with connections via optically coupled isolation amplifiers. Measurements of the junction's voltage noise spectrum showed no peak at 60 Hz and its harmonics. Extensive diagnostic tests were performed using low critical current junctions ($I_c \sim$ 1 to 10 μA) to ensure that extrinsic noise from the measurement circuit was negligible down to 10 mK.

The conventional method of measuring escape probability P_{esc} versus bias current cannot provide information about the time dependence of P_{esc} at constant i_b, so we have developed a time-domain technique with nanosecond resolution for $P_{esc}(t)$ measurement. For each escape event, we started the cycle by ramping up the bias current to a constant value i_b where escape rate was negligibly small. The bias current was maintained at this level for a short time (~10^{-3} s) to allow the system to reach thermal equilibrium. Using a pulse generator, a "dc pulse" of amplitude Δi_b and width $t_{PLS} \leq 1$ μs was then applied to the junction at $t = -t_{PLS}$ (Fig. 2). The pulse produced a nonequilibrium popula-

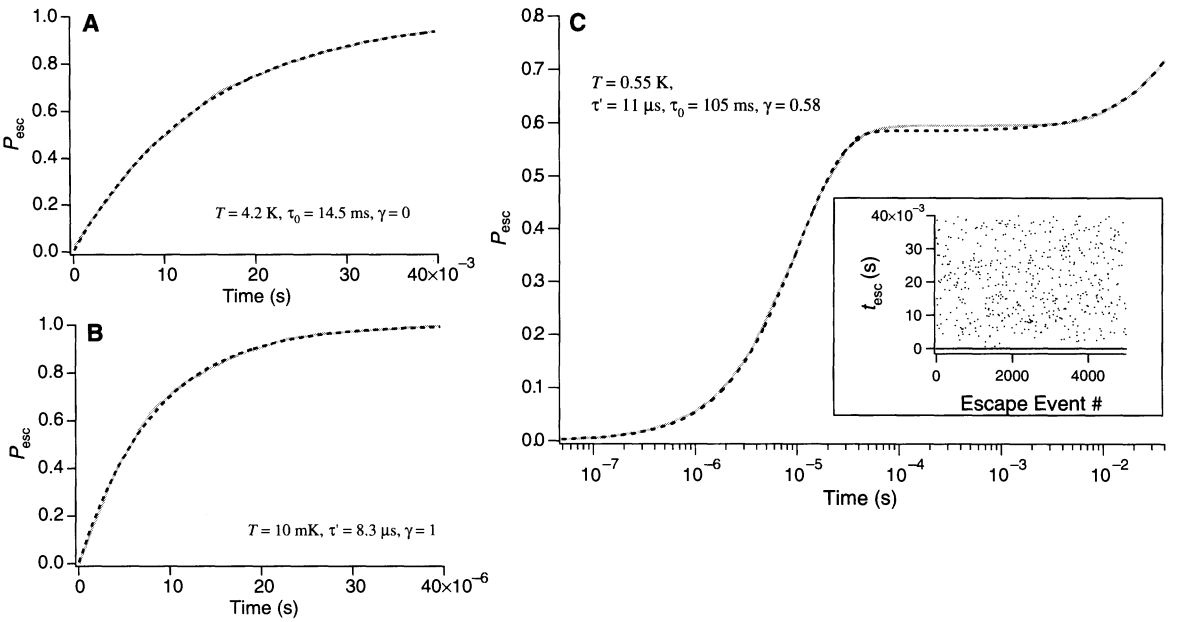

Fig. 3. Data (solid lines) of escape probability taken at (**A**) T = 4.25 K, (**B**) 0.01 K, and (**C**) 0.55 K. The dashed lines are the best fit to exponential behavior with a single (two) rate constant(s). The escape time of each event, at T = 0.55 K, is shown in the inset of (C). Bias current for (B) was slightly larger than for (C), resulting in a faster tunneling rate.

tion $\rho_{11}(0)$ through a mechanism similar to Majorana oscillation (*29*). The $\rho_{11}(0)$ can be estimated by considering the time evolution of a two-level system under a constant perturbation for a time period t_{PLS}. The Liouville equation of the time evolution of the density matrix operator, including the effects of decay and tunneling rates (Γ_d, Γ_0, and Γ_1), can be analytically solved by using the Laplace transformation, from which the time-dependent population of both levels can be obtained. The analytical expression, which is rather complicated, will be described in detail elsewhere. In the limit of Γ_d, $\Gamma_1 \ll t_{PLS}^{-1}$ a simple analytical solution can be obtained

$$\rho_{11}(0) = \frac{\chi^2}{\chi^2 + \omega^2} \sin^2\left(\sqrt{\chi^2 + \omega^2}\,\frac{t_{PLS}}{2}\right) \quad (3)$$

Here, $\hbar\omega = E_1 - E_0$ is the level spacing, $\chi = 2V_{01}/\hbar$ and V_{01} is the coupling between the two levels by the "dc pulse." The formula shows that the maximum excitation probability to the upper level is always less than unity but can be quite substantial.

The junction voltage was fed to a timer that was triggered by the sudden voltage jump when the junction switched from the zero-voltage to the finite-voltage state, to record t_{esc} (Fig. 2). i_b was then decreased to zero, resetting the junction to the zero-voltage state. The process was repeated $\sim 10^4$ times to obtain $P_{esc}(t)$.

Data were taken at T = 4.2, 0.01, and 0.55 K (Fig. 3). As expected, at the high- and low-temperature limits, the measured $P_{esc}(t)$ exhibits single-exponential behavior. In contrast, the data at T = 0.55 K display the double-exponential behavior characteristic of a TLDT process (Fig. 3C). We emphasize that this double-exponential behavior was reproducible as long as the junction was well shielded from extrinsic noises. The values of γ, $\tau_0 \equiv 1/\Gamma_0$, and $\tau' \equiv 1/\Gamma'$ obtained from the best fit are 0.58, 0.105 s, and 0.011 ms, respectively. Therefore, $\tau_d > 11$ μs, corresponding to a minimum "effective damping resistance" $R \simeq 2$ megohms according to Eq. 2. Note that the quasi-particle subgap resistance of an ideal NbN tunnel junction $R_{qp} \sim R_n e^{\Delta/k_B T} \sim 10^{25}$ ohms $\gg R$, indicating nonideal nature of the junction and the presence of other sources of dissipation (*4*). Notice that it is difficult to use this method to determine τ_d at low temperatures where $\Gamma_d \ll \Gamma_1$ unless $\rho_{11}(0)$ can be independently determined. Therefore, although it is expected that R could be greater than 2 megohms at $T \ll 0.5$ K it cannot be quantitatively verified. The data in Fig. 3, B and C, also demonstrate the nanosecond resolution of our time-domain measurement technique that opens the door to the study of temporal evolution of Josephson junctions and SQUID qubits.

In addition to τ_d, τ_φ also depends on R. For typical rf SQUID qubits

$$\tau_\varphi \simeq (\pi\alpha k_B T)^{-1} \simeq 1.5\frac{R/1\,\text{megohms}}{T/1\,mK} \quad (4)$$

where α is the quantum damping parameter (*18*) and τ_φ is in μs. For rf SQUIDs of 1 μm^2 junctions having specific resistance, R_s = 0.2 gigohms · μm^2, the most conservative estimate gives $\tau_\varphi \approx 30$ μs at 10 mK, a figure very promising for QC (*12*).

References and Notes

1. D. Loss, D. P. DiVincenzo, *Phys. Rev. A* **57**, 120 (1998).
2. B. Kane, *Nature* **393**, 133 (1998).
3. M. F. Bocko, A. M. Herr, M. J. Feldman, *IEEE Trans. Appl. Supercon.* **7**, 3638 (1997).
4. T. P. Orlando *et al.*, *Phys. Rev. B* **60**, 15398 (1999).
5. J. R. Friedman, V. Patel, W. Chen, S. K. Tolpygo, J. E. Lukens, *Nature* **406**, 43 (2000).
6. C. H. van der Wal *et al.*, *Science* **290**, 773 (2000).
7. A. Shnirman, G. Schijn, Z. Hermon, *Phys. Rev. Lett.* **79**, 2371 (1997).
8. D. V. Averin, *Solid State Commun.* **105**, 659 (1998).
9. Y. Nakamura, Y. A. Pashkin, J. S. Tsai, *Nature* **398**, 786 (1999).
10. D. J. Flees, S. Han, J. E. Lukens, *J. Supercon.* **12**, 813 (1999).
11. G. M. Palma, K. A. Suominen, A. K. Ekert, *Proc. R. Soc. London A* **452**, 567 (1996).
12. M. A. Nielsen, I. L. Chuang, in *Quantum Computation and Quantum Information* (Cambridge Univ. Press, Cambridge, ed. 1, 2000), chap. **7**.
13. M. B. Plenio, P. L. Knight, *Proc. R. Soc. London A* **453**, 2017 (1997).
14. W. H. Zurek, *Phys. Today* **44** (no. 10), 36 (1991).
15. D. Braun, F. Haake, W. T. Strunz, *Phys. Rev. Lett.* **86**, 2913 (2001).
16. M. B. Plenio, P. L. Knight, *Phys. Rev. A* **53**, 2986 (1996).
17. A. I. Larkin, Y. N. Ovchinnikov, *Sov. Phys. JETP* **64**, 185 (1986).
18. A. J. Leggett *et al.*, *Rev. Mod. Phys.* **59**, 1 (1987).
19. C. Cosmelli *et al.*, *Phys. Rev. Lett.* **82**, 5357 (1999).
20. S. Han, R. Rouse, *Phys. Rev. Lett.* **86**, 4191 (2001).
21. J. Clarke, A. N. Cleland, M. H. Devoret, D. Esteve, J. M. Martinis, *Science* **239**, 992 (1988).
22. J. M. Martinis, M. H. Devoret, J. Clarke, *Phys. Rev. Lett.* **55**, 1543 (1985).
23. J. M. Schmidt, A. N. Cleland, J. Clarke, *Phys. Rev. B* **43**, 229 (1991).
24. W. Bialek, S. Chakravarty, S. Kivelson, *Phys. Rev. B* **35**, 120 (1987).
25. P. Silvestrini, V. Palmieri, B. Ruggiero, M. Russo, *Phys. Rev. Lett.* **79**, 3046 (1997).
26. Z. Wang, H. Terai, A. Kawakami, Y. Uzawa, *Appl. Phys. Lett.* **75**, 701 (1999).
27. J. P. Kauppinen, J. P. Pekola, *Phys. Rev. Lett.* **77**, 3889 (1996).
28. A. B. Zorin, *Rev. Sci. Instrum.* **66**, 4296 (1995).
29. B. W. Shore, *Simple Atoms and Fields*, vol. 1 of *The Theory of Coherent Atomic Excitation* (Wiley, New York, 1990).

30. S.H. is grateful to J. Lukens, D. Averin, and J. Martinis for stimulating comments and suggestions. The authors also acknowledge Y. Zhang, V. Patel, W. Qiu, L. Olafsen, and S. Li for technical assistance. This work was supported in part by the U.S. Air Force Office of Scientific Research (F49620-99-1-0205), the State of Kansas (S99041), and NSF (DMR9876874 and EIA0082499).

4 May 2001; accepted 24 July 2001